Liquid Crystals
Publication details, including instructions for authors and subscription information:
http://www.informaworld.com/smpp/title~content=t713926090

Droplet-size distribution gradient induced by laser curing in polymer dispersed liquid crystals

D. E. Lucchetta; O. Francescangeli; L. Lucchetti; F. Simoni

Online publication date: 06 August 2010

To cite this Article Lucchetta, D. E. , Francescangeli, O. , Lucchetti, L. and Simoni, F.(2001) 'Droplet-size distribution gradient induced by laser curing in polymer dispersed liquid crystals', Liquid Crystals, 28: 12, 1793 — 1798
To link to this Article: DOI: 10.1080/02678290110078784
URL: http://dx.doi.org/10.1080/02678290110078784

LIQUID CRYSTALS, 2001, VOL. 28, NO. 12, 1793–1798

Droplet-size distribution gradient induced by laser curing in polymer dispersed liquid crystals

D. E. LUCCHETTA, O. FRANCESCANGELI*, L. LUCCHETTI and F. SIMONI

Dipartimento di Fisica e Ingegneria dei Materiali e del Territorio and Istituto Nazionale per la Fisica della Materia,
Università di Ancona, Via Brecce Bianche, I-60131 Ancona, Italy

(*Received 28 April 2001; in final form 4 June 2001; accepted 14 June 2001*)

We have studied the morphology and electro-optical properties of polymer dispersed liquid crystals prepared by polymerization-induced phase separation (PIPS) under high intensity UV laser curing. The results have shown that localized high intensity curing generates a gradient of the droplet size distribution outside the directly irradiated area as a consequence of the non-uniform spatial distribution of the scattered intensity. Such a distribution of the droplet size reflects in a peculiar electro-optical behaviour that could find potential application in optical devices. Both shape and spatial extent of the droplet size gradient are affected by the spatial velocity of polymerization which in turn strongly depends on the intensity of the curing laser beam. This dependence has also been experimentally investigated.

1. Introduction

Polymer dispersed liquid crystals (PDLCs) are composite materials in which nematic liquid crystals (NLCs) are phase-dispersed as micro-sized droplets in a polymer matrix [1]. These materials have received much attention in recent years because of their great potentialities in electro-optical applications, as well as in storage devices and non-linear optical elements [2].

PDLCs have been described extensively in the literature [3–5]. They operate on the basis of the refractive index mismatch between the NLC and the polymer matrix. The NLCs used have generally a positive dielectric anisotropy and therefore align with their director parallel to an electric field; they are selected so that their ordinary refractive index (n_0) matches the refractive index of the polymer matrix. Thus, the film is normally scattering because of random orientation of n_0 in the absence of an electric field, but becomes transparent when such a field is applied, since the LC alignment provides an effective refractive index that is the same for matrix and droplets.

PDLCs are generally obtained by phase separation of the liquid crystal from the polymeric network. Phase separation can be induced by polymerization (polymerisation-induced phase separation: PIPS), thermal quenching (thermal-induced phase separation: TIPS) or solvent evaporation (solvent-induced phase separation: SIPS) [6]. In the PIPS process activated by incoherent UV radiation, the separation of the LC droplets is induced by photopolymerization and crosslinking of a polymer precursor mixed with the LC. In PIPS, phase separation occurs with the progress of polymerization due to the unfavourable increase in the Gibbs free energy of mixing resulting from the decrease in the entropy of mixing since progressively smaller numbers of molecules become involved. These PDLC samples are characterized by well defined distribution functions of the LC droplet size which have been characterized recently [7].

PDLC samples cured by low intensity coherent laser radiation exhibit a similar behaviour; however, high intensity coherent laser curing may give rise to completely new morphologies. A few authors have performed studies on laser curing of PDLCs. Among them, Fuh and Caporaletti have analysed in detail the dependence of droplet size and distribution both on the curing rate and the density ratio of the polymer, showing that faster curing leads to smaller droplets and that a density ratio close to unity improves the distribution uniformity of the samples [8]. Sutherland and co-workers have published several papers dealing with the writing of high resolution gratings in PDLCs during the curing process [9–12] and Simoni and co-workers showed how to use the laser curing process to store binary images in these materials [13]. Although all of these papers are exhaustive in describing some aspect of the coherent curing, the dependence of both the morphology and the size distribution on the intensity of the laser radiation is a subject of investigation still widely unexplored. With the aim of

*Author for correspondence; e-mail: france@popcsi.unian.it

Liquid Crystals ISSN 0267-8292 print/ISSN 1366-5855 online © 2001 Taylor & Francis Ltd
http://www.tandf.co.uk/journals
DOI: 10.1080/02678290110078784

providing new insight into this field we have recently started a systematic study of the effects of the intensity of coherent radiation on the morphology of PDLC samples. We have characterized samples cured by UV light with intensity varying from $\approx 300\,\mathrm{mW\,cm^{-2}}$ to $\approx 20\,\mathrm{W\,cm^{-2}}$. The experimental results have revealed an extremely interesting and unexpected sample morphology in the region directly illuminated by the beam, which involves the formation of peculiar *disordered* or *ordered* structural patterns. In both cases, the resultant irradiated region is transparent to visible light: in the former case this occurs because of the formation of submicron-sized LC domains that do not scatter the visible light; in the latter case, the reason for the transparency lies in the alignment of the LC molecules along a preferential direction. The observed complex phenomenology, which is very attractive for applications in the field of molecular micro-assembly and self-ordering structures, has been reported and discussed in detail in a previous paper [14].

In this communication we report the study of the PDLC morphology and related electro-optical properties of the sample outside the irradiated area. The dependence of these properties on the intensity of the coherent UV light is also investigated. The experimental results indicate that localized high intensity curing generates a gradient of the droplet size distribution as a consequence of the non-uniform spatial distribution of the scattered intensity and of the thermal gradients around the irradiated area. Such a distribution of the droplet size reflects in a peculiar electro-optical behaviour that could find potential application in optical devices. Both the shape and spatial extent of droplet size gradient are strongly affected by the velocity of polymerization which in turn depends on the intensity of the curing laser beam. This dependence has also been investigated in this study by means of a specifically designed experimental set-up.

2. Experimental results and discussion

The PDLC samples were prepared as thin films using two conductive glass plates (3 cm × 1.5 cm × 0.1 cm) filled by capillarity with a 1:1 weight-ratio mixture of the nematic liquid crystal E7 (Merck) and NOA65 (Norland), a UV photocurable commercial optical adhesive. The cell thickness was 23 μm. Samples were fixed in the vertical position and were irradiated with an Ar^+ laser beam ($\lambda = 333.6$–363.8 nm) which impinged perpendicularly on the glass plates. Temperature was set at 30°C (stability ±0.1°C), exposure time was fixed at 30 s and light power was varied in the range 6–400 mW. No electric field was applied during irradiation. The diameter of the laser beam on the sample was 1.5 mm. The conductive glasses absorbed more than 30% of the incident light in the wavelength range explored [15].

The light transmitted through the glass excites the photoinitiators, initiating a fast polymerization process, with consequent phase separation of the LC. A description of the chemical reactions involved in the photopolymerization process for the NOA65-E7 mixture is reported in [15]. Due to the scattered light, the polymerization and phase separation processes extend outside the directly illuminated area. Once the LC domains start to form in the illuminated area, the material scatters laser light in all directions. The polymerization rate depends on the intensity I of the UV light and is higher where I is higher. As the intensity of the scattered light is inversely proportional to the square of the distance r from the centre of the irradiated spot, the polymerization rate in the sample changes with r depending on the local value of the intensity. In addition to the scattered intensity, diffusion phenomena involving migration of both excited photoinitiators and monomers from the central region of the beam to the outer region are expected to affect the polymerization rate, especially close to the direct beam where thermal gradients are stronger. However, diffusion of low molecular mass species through the polymer greatly depends on the viscosity of the polymer which in turn depends on the degree of polymerization. As the starting isotropic mixture is rather viscous, and considering that the polymerization proceeds very quickly just in the region where the gradients are stronger, the latter effect plays a minor role in determining the rate of polymerization. So, polymerization and consequent phase separation processes of the LC proceed more and more slowly with increasing r, and therefore a delay time Δt occurs between the formation of the polymeric network at two points separated by Δr. From a macroscopic point of view, polymerization appears to start from the centre of the spot and to propagate in the plane parallel to the glass substrates, with circular symmetry. We define the spatial velocity of polymerization u as the propagation velocity of the polymeric network, i.e. the limit of the ratio $\Delta r/\Delta t$ when the distance Δr becomes arbitrarily small.

The morphological properties of PDLCs submitted to different curing intensities were analysed by optical microscopy. For all the investigated samples, a *droplet* morphology of the dispersed LC domains was found outside the irradiated region. A typical example is shown in figure 1.

The continuous regular increase of the average droplet radius that is observed on moving away from the laser spot is intimately connected with the curing technique. In fact, the photo-polymerization process outside the irradiated volume of the sample is activated by the light scattered from the high power direct beam and is also affected by the thermal gradients originated by the high intensity local curing. The intensity of the scattered UV

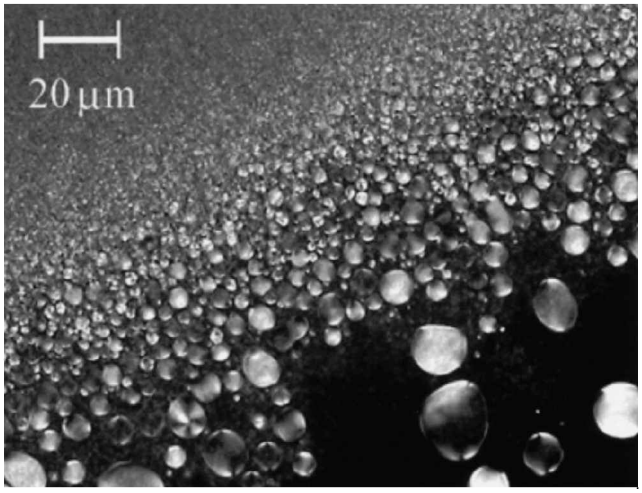

Figure 1. Optical micrograph of the PDLC film. The figure shows a typical example of the droplet morphology and the droplet size gradient distribution existing outside the directly illuminated area. The picture is taken at a distance of 1.5 cm from the centre of the spot, close to the border of the polymerized area.

light decreases with the distance from the illuminated region. As the average droplet size decreases with increasing the curing intensity, this leads to the observed radial distribution where the average droplet radius is approximately inversely proportional to the local curing intensity. In summary, the radial intensity gradient originated by the laser beam generates in turn a droplet size gradient of opposite sign where the droplet dimension increases with the distance from the laser spot. The spatial extension of this gradient has been found to be dependent on the intensity of the direct beam, mainly because of the intensity dependence of the propagation velocity of the polymerization process.

The spatial velocity of polymerization close to the illuminated area was measured by means of the experimental set-up shown in figure 2. The incident low power He-Ne laser beam probe was split into two identical beams (1.5 mm spot size) impinging on the sample at two points, A and B, located at different distances from the pump-beam spot. After crossing the cell, the two probe beams were collected by a large-area photodetector that allowed measurement of the time evolution of the PDLC transmittance under a given curing intensity. The finite speed of polymerization u was monitored by the time evolution of the transmission curve. It is important to observe here that this technique actually gives the propagation velocity of the phase separation process and this velocity may not coincide with u. In fact, with a rapid enough rate of polymerization, phase separation cannot follow the polymerization kinetics since the time scale for polymerization is smaller and that of phase separation becomes larger due to the slower diffusion of the LC molecules in the highly viscous media. However, the polymerization rate outside the directly irradiated area is far from this condition in our experiment, and therefore the two velocities can be assumed to coincide.

In figure 3 we report a set of transmittance vs. curing time curves obtained for different values of the curing power. These were measured with the two He-Ne probes at $r_A = 2$ mm and $r_B = 4.5$ mm from the centre of the Ar^+ spot. As a general trend, these curves exhibit with increasing time a decreasing behaviour characterized by an alternation of flat regions and smooth slopes. Such behaviour can be explained by the growth of the polymeric network, which affects regions located farther and farther away as the polymerization proceeds. In particular, the two smooth slopes correspond to the crossing of the He-Ne spots by the wavefront of the advancing polymeric network, whereas the flat regions correspond to the propagation of the network between two successive spots. In fact, the PIPS process creates small randomly oriented micron-sized LC domains that strongly scatter visible light, so reducing the transmitted intensity. On increasing the curing power, the slopes become steeper and steeper and the width of the flat regions correspondingly reduces. Both effects clearly indicate an increase in the spatial polymerization velocity due to the higher curing laser intensity. The sharp initial

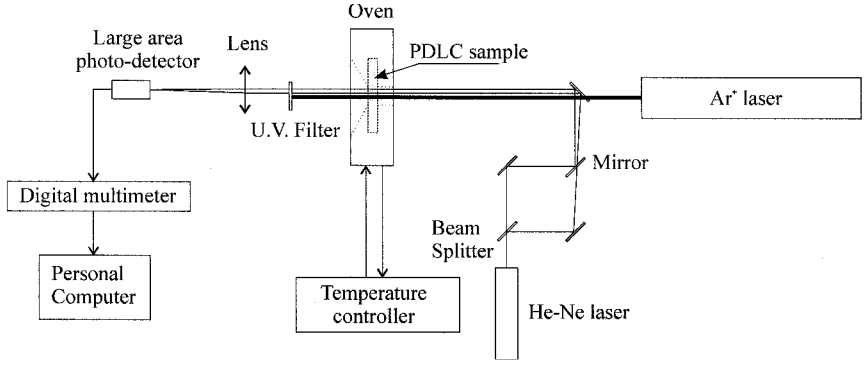

Figure 2. Experimental set-up for the measurement of the spatial velocity of polymerization.

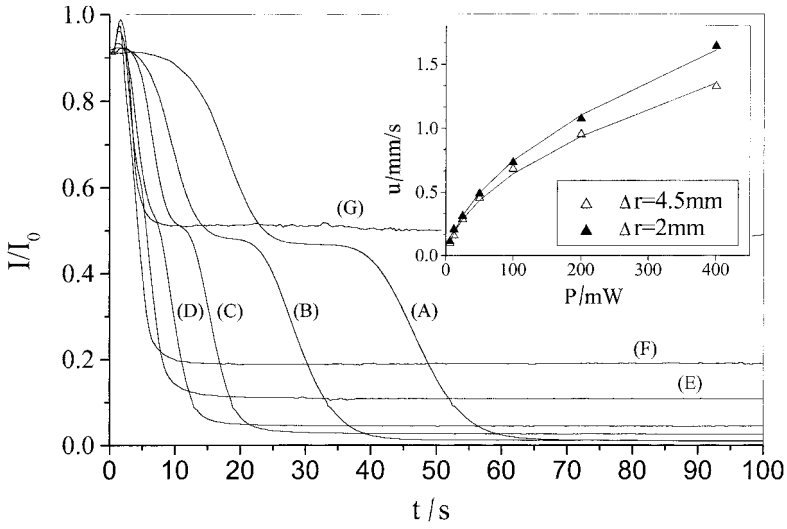

Figure 3. Transmittance of the PDLC film vs. curing time for different values of the curing power: (A) 6 mW; (B) 12 mW; (C) 25 mW; (D) 50 mW; (E) 100 mW; (F) 200 mW; (G) 400 mW. The inset reports the spatial velocity of polymerization u as a function of the curing power: the symbols (▲) and (△) refer to the He-Ne spots located at $r_A = 2$ mm and $r_B = 4.5$ mm, respectively, from the centre of the Ar^+ spot.

peak observed for high pump laser powers (higher than about 25 mW) and the increase in the asymptotic value of the transmittance are both due to the scattering of UV radiation that increases with the Ar^+ laser intensity.

The experimental data made it possible to make a quantitative determination of the average spatial polymerization velocity and its dependence on the pump intensity. The difference in the slopes corresponding to the two He-Ne spots for a given laser intensity indicates a continuous reduction of the polymerization speed on moving away from the irradiated region. The inset of figure 3 shows the spatial velocity of polymerization u as a function of the curing power. The two curves refer to the average velocities calculated in the two adjacent time intervals corresponding to the travelling distance between the consecutive spots. The lowering of u with increase of the distance r from the Ar^+ spot is due to the reduction of the Ar^+ light intensity, whereas the increase of u with the laser power is connected with the higher polymerization rate. The two curves in the inset of figure 3 can be satisfactorily fitted by assuming a square root dependence of u on the curing power. Since the phase separation is driven by the polymerization reaction, the rate of polymerization for a photoinitiated radical mechanism largely governs the phase separation and hence the domain size.

We have seen in the Introduction that droplet formation proceeds from both activation via indirect light scattering and radical propagation. If, to a first approximation and based on the previously reported considerations, we neglect the effects of the latter process we can justify this experimental finding by assuming for the local polymerization rate R a square root dependence on the incident light intensity, similar to that holding for photoinitiated free radical systems [16].

$$R = K_p[M]\left(\frac{\phi\varepsilon I[A]v}{K_t}\right)^{1/2} \tag{1}$$

where I is the intensity of the incident curing light, [M] and [A] are the concentrations of monomer and of species which undergo photoexcitation, ϕ is the initiation efficiency, ε the molar absorptivity, v the fraction of initiator fragments that successfully react with the monomer, and K_p and K_t are the rate constants for the propagation and termination reactions, respectively.

Because of the different distances of A and B from the centre of the irradiation spot, the intensities of the UV scattered light at A and B are in the ratio $I_A/I_B = (r_B/r_A)^2$. According to equation (1), and assuming a uniform spatial distribution of the mixture components, the time t to get complete polymerization at a given r is inversely proportional to the local polymerization rate. So the times t_A and t_B needed to complete polymerization at A and B are in the ratio $t_A/t_B = R_B/R_A = (I_B/I_A)^{1/2} = r_A/r_B$, where R_A and R_B are the polymerization rates at A and B, respectively. The average propagation velocity u of the polymeric network between A and B is then

$$u = \frac{r_A - r_B}{t_A - t_B} = \frac{r_A}{t_A}\frac{(1 - r_B/r_A)}{(1 - t_B/t_A)} = \frac{r_A}{t_A}. \tag{2}$$

Considering that $I_A = I/r_A^2$, where I is the intensity of the direct beam, and that t_A is inversely proportional to

R_A, equations (2) and (1) give

$$u \propto r_A R_A = const \quad r_A I_A^{1/2} = const \quad I^{1/2} \qquad (3)$$

where *const* indicates a proportionality constant depending on the physicochemical parameters of the system. Thus, within our simplified model, the observed dependence of u on the square root of the curing power reflects the dependence on $I^{1/2}$ of the polymerization rate.

The electro-optical properties were studied by submitting the sample to an external voltage V and measuring the transmission of a He-Ne laser beam probe (1.5 mm diameter) at different points of the sample. An interesting behaviour was observed that is connected with the peculiar morphology of these samples. Figure 4 shows a three-dimensional (3D) representation of the transmission properties of a PDLC film for different values of the applied voltage V.

The sample investigated was prepared by UV curing at the relatively low intensity of 680 mW cm^{-2}. Under these conditions the droplet morphology extends slightly into the directly illuminated volume (close to the border) and the same is true for the droplet size gradient distribution. Figures 4(*a–c*) report the 2D intensity profiles of the transmitted probe beam corresponding to 10, 30 and 80 V as detected by a CCD camera with the photosensitive surface orthogonal to the propagation direction. This figure refers to a situation where the probe-beam was centred right in the centre of the illuminated area (i.e. the centre of the pump laser beam). For the sake of comparison, in figure 4(*d*) the radial intensity profiles of the transmitted beams are compared with that of the incident gaussian beam (full line). In this latter figure the intensity of the incident beam is normalized to the peak intensity of the curve at 80 V. At low voltages, figure 4(*a*), the transparent area of the film is smaller than the directly illuminated area and the cross-section of the transmitted beam is smaller than that of the incident beam. On increasing the voltage, the transparent region extends outside the directly illuminated area, with circular symmetry. However, points located farther away become more transparent at lower voltages than points located closer to the centre of the Ar^+ beam. In other words, a continuous widening of the transparency area is observed on increasing V, and this proceeds radially from outer to inner regions, figures 4(*b*, *c*). This behaviour can be explained in terms of the droplet size gradient distribution existing close to the border and outside the area directly illuminated by the incident

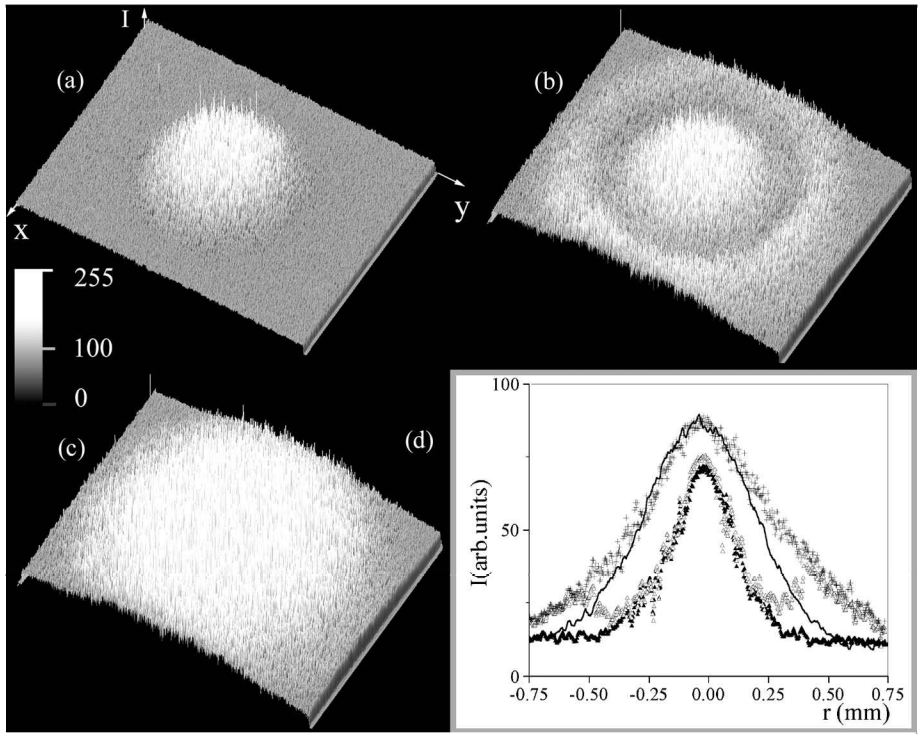

Figure 4. 3D representation of the transmission properties of a PDLC film for different values of the applied voltage V. The curing intensity is 680 mW/cm^2. Figures 4(*a–c*) report the 2D intensity profiles $I(x, y)$ of the transmitted beam, corresponding to 10 V (*a*), 30 V (*b*), and 80 V (*c*), respectively, as detected by a CCD camera. The horizontal plane xy is a cross-section of the beam, while the vertical axis I gives the beam intensity. Figure 4(*d*) shows the radial intensity profiles (symbols) for the cases (*a–c*) compared with that of the incident gaussian beam (full line): 10 V (▲); 30 V (△); 80 V (+). r is the radial distance from the centre of the Ar^+ spot. The intensity of the incident beam is normalized to the peak intensity of the curve at 80 V.

beam. In fact, the reorientation field E (voltage/film thickness) of a PDLC film is related to the curvature radius ρ of the nematic director. Under strong anchoring conditions, an estimate of this dependence can be obtained through the following approximate relation [2, 17]:

$$E \approx \frac{1}{\rho}\left(\frac{K}{\varepsilon_0 \Delta\varepsilon}\right)^{1/2} \tag{4}$$

where K is an elastic constant, $\Delta\varepsilon$ is the dielectric anisotropy and, for spherical droplets, ρ is simply the droplet radius R. According to equation (4) the reorientation field is expected to scale inversely with droplet size so that smaller droplets require higher fields to be reoriented. In the case of figure 4 (*a*) the electric field is insufficient to reorient any of the LC droplets outside the irradiated region. In the case of figure 4 (*b*) the field is strong enough to reorient the LC droplets with larger radius, i.e. those that are farther from the centre of the spot. Finally, in the case of figure 4 (*c*) the electric field becomes sufficient to reorient all the droplets, and the whole area surrounding the central spot becomes transparent. Thanks to this peculiar electro-optical behaviour, it is possible to control both the spatial extension and the intensity profile of the transmitted beam. The application of a time-dependent voltage in the form of a slow ramp leads to a *wipe* effect consisting of the continuous radial advance of the transparency wavefront, with a velocity that depends on the slope of the ramp. Similarly, application of a low frequency sinusoidal electric field gives rise to a modulated reversible *iris* effect.

The same electro-optical behaviour was observed for samples cured at higher intensities. However, on increasing the intensity, the thermal effects on the droplet size distribution become stronger. In particular, the temperature of the sample in the region of the tail of the gaussian incident beam increases, and this favours the formation of a ring close to the border of the spot with a droplet morphology characterized by very small radii. These droplets are small enough to require very high fields for reorientation, but at the same time are big enough to scatter the visible light. Accordingly, this ring remains opaque under any applied voltage lower than 100 V (i.e. the maximum value allowed by our experimental set-up). For higher curing intensities, however, the inner spot is brighter than that obtained at low curing intensities. So in practical applications a compromise has to be reached between the requirements of high transparency and reasonable reorienting fields.

3. Conclusions

In this paper we report the first study outside the directly irradiated area of the morphology and related electro-optical properties of polymer dispersed liquid crystals prepared by the polymer-induced phase separation (PIPS) technique activated by high intensity coherent laser light. The measurement of the spatial velocity of polymerization and its dependence on the curing intensity is also reported. The experimental results indicate that localized high intensity curing generates a gradient of the droplet size distribution as a consequence of the non-uniform spatial distribution of the scattered intensity and of the thermal gradients. The observed distribution of droplet size is manifest in a peculiar electro-optical behaviour that could find application in optical devices. We think that the results of this study may stimulate further investigation by scientists involved in the same or closely connected research subjects and lead to fruitful results both from a theoretical and an applicative point of view.

References

[1] Doane, J. W., Vaz, N. A., Wu, B. G., and Zumer, S., 1986, *Appl. Phys. Lett.*, **48,** 269.

[2] Simoni, F., and Francescangeli, O., 2000, *Int. J. polym. Mater.*, **45,** 381 and refs. quoted therein.

[3] Draizc, P. S., 1986, *J. appl. Phys.*, **60,** 2142.

[4] Zumer, S., and Doane, J. W., 1986, *Phys. Rev. A.*, **43,** 3373.

[5] Wu, B. G, West, J. L., and Doane, J. W., 1987, *J. appl. Phys.*, **62,** 3925.

[6] West, J. L., 1988, *Mol. Cryst. liq. Cryst.*, **157,** 427.

[7] Lucchetti, L., and Simoni, F., 2000, *J. appl. Phys.*, **88,** 3934.

[8] Fuh, A., and Caporaletti, O., 1989, *J. appl. Phys.*, **66,** 5278.

[9] Sutherland, R. L., Tondiglia, V. P., Natarajan, L. V., Bunning, T. J., and Adams, W. W., 1994, *Appl. Phys. Lett.*, **64,** 1074.

[10] Tondiglia, V. P., Natarajan, L. V., Sutherland, R. L., Bunning, T. J., and Adams, W. W., 1995, *Opt. Lett.*, **20,** 1325.

[11] Bunning, T. J., Natarajan, L. V., Tondiglia, V. P., Sutherland, R. L., Vezie, D. L., and Adams, W. W., 1995, *Polymer*, **36,** 2699.

[12] Sutherland, R. L., and Natarajan, L. V., 1997, *Liq. Cryst.*, **7**, 1.

[13] Di Bella, S., Lucchetti, L., and Simoni, F., 1999, *Mol. Cryst. liq. Cryst.*, **336,** 247.

[14] Lucchetta, D. E., Francescangeli, O., Lucchetti, L., and Simoni, F., 2001, *Mol. Cryst. liq. Cryst.* (in the press).

[15] Lucchetta, D. E., Lucchetti, L., Gobbi, L., and Simoni, F., 2001, *Mol. Cryst. liq. Cryst.*, **360,** 81.

[16] Odian, G., 1981, *Principles of Polymerisation* (New York: Wiley).

[17] Draizc, P. S., 1995, *Liquid Crystals Dispersions* (Singapore: World Scientific).